Journal of Molecular Modeling (2022) 28: 97
https://doi.org/10.1007/s00894-022-05090-2

ORIGINAL PAPER

First-principles study on electronic and optical properties of single-walled carbon nanotube under an external electric field

Omar Bajjou[1,5] · Abdelhafid Najim[2] · Khalid Rahmani[3] · Mohammed Khenfouch[4,5]

Received: 3 October 2021 / Accepted: 11 March 2022 / Published online: 23 March 2022

Abstract

In this study, the electronic and optical properties of one-dimensional (1D) single-walled carbon nanotube (SWCNT) nanostructures, and under the external electric field (E_{ext}) applied in the z-direction, are investigated using density functional theory (DFT) calculations. The applied E_{ext} leads to significant modulation of the bandgap and changes the total density of states (TDOS), partial density of states (PDOS), absorption coefficient, dielectric function, optical conductivity, refractive index, and the loss function. The application of the E_{ext} on the SWCNT/Carboxyl structure leads to tighten its bandgap. The peaks of TDOS around the Fermi level are very weak. The absorption coefficient increases in visible range and decreases in ultraviolet (UV) domain proportionally with the E_{ext}. It is found that electronic structures and optical properties of the SWCNT/Carboxyl could be affected by the E_{ext}. All these results provide the important information for understanding and controlling the electronic and optical properties of 1D crystals by the E_{ext}. This study establishes a theoretical foundation for our future experimental work regarding optoelectronic properties of the SWCNT/Carboxyl material.

Keywords External electric field · Optical property · First-principles calculation · Electronic structure · Absorption spectrum

Introduction

The tight binding Hamiltonian of π electrons in carbon atoms accurately describes the electronic states of graphene [1]. Carbon atoms forming the graphene have four valence electrons that occupies 2 s and 2p orbitals ($2s^2\ 2p^2$). In the graphene, three atomic orbitals 2 s, $2p_x$, and $2p_y$ are hybridized to form three sp^2 hybrid orbitals in the same plane; the $2p_z$ orbital, on the other hand, remains perpendicular to the other orbitals. Three σ bonds between neighboring carbon atoms are formed by hybridized orbitals, while π bonds outside the plane of the graphene sheet are formed by $2p_z$ orbitals [2]. Furthermore, graphene is a semimetal with zero bandgap energy, and it is one prominent 2D material that has received a lot of attention in many fields due to its exceptional physical properties. Its band structure has a zero gap at the Dirac point, which can be widened by external disturbances such as the E_{ext} [3].

The graphene can be considered the elementary unit of three carbon allotropes, graphite, buckyball, and carbon nanotubes that are formed by folding the graphene into a cylinder [4]. In recent years, the carbon nanotubes have been intensively studied due to their importance as building block in nanotechnology. Three different carbon nanotube structures are experimentally observed: armchair, zigzag, and chiral [5, 6]. Furthermore, thanks to their cylindrical shape and large specific surface area as well as their chirality, the CNTs (carbon nanotubes) can strongly interact with light, and provide

✉ Omar Bajjou
bajjou.omar@gmail.com

Abdelhafid Najim
najim.phymo@gmail.com

1 Energy and Materials Engineering Laboratory "LGEM", Faculty of Sciences and Technics, Sultan Moulay Slimane University, BP 523, 23000 Beni Mellal, Morocco

2 LDD, Faculty of Sciences and Technics, Sultan Moulay Slimane University, BP 523, 23000 Beni Mellal, Morocco

3 Research Laboratory in Physics and Sciences for Engineers (LRPSI), Poly-disciplinary Faculty, Sultan Moulay Slimane University, Beni Mellal, Morocco

4 Faculty of Applied Sciences, Ibn Zohr University, Ait Melloul, Morocco

5 UNESCO UNISA Africa Chair in Nanosciences & Nanotechnology (U2ACN2), College of Graduate Studies, University of South Africa (UNISA), Pretoria, South Africa

exceptional electronic and optical properties making them promising materials for applications in the fields of nanoelectronics and energy storage [7, 8]. The electronic properties of the CNTs are due to the sp^2-hybridized carbon atoms and delocalized π network perpendicular to the nanotube surface [9]. With a large surface area all carbon atoms could be in direct contact with the external exposed molecules. Additionally, they are very sensitive to the surrounding environment and they could be suitable for storing molecules adsorbed on the surface. A carboxyl unit substitution on the surface creates the specific group (-C(=O)OH) with sp^3 carbon regions [10].

In general, the E_{ext} leads to a change in the carrier concentration in a semiconductor material, by modifying the electric current, and it also alters the electronic and optical responses of 1D-SWCNT. The study of external electric field impact on SWCNT/Carboxyl structure's electrical and optical properties has known a considerable interest in research and development, thanks to the important changes observed in the electro-optical properties [11, 12].

The present study addresses the E_{ext} applied in the z-direction on the SWCNT/Carboxyl using first-principles calculations, along with discussions on the results concerning the electronic structure and optical properties of this 1D material [13], as well as the bandgap energy evolution, TDOS, PDOS, and optical properties. However, in the case of the application of the E_{ext} a perturbation in the form of electrostatic potential to the Hamiltonian of π-electrons in the SWCNT/Carboxyl structure is expected. The homogeneous E_{ext} leads to modify the Hamiltonian of the SWCNT/Carboxyl structure:

$$H = H_0 - eE_z \tag{1}$$

where H_0 is the Hamiltonian of the system in equilibrium conditions.

In the absence of an E_{ext}, the dependence between electronic properties and geometric structure can clearly be seen in both state and the value of the bandgap energy. The zigzag nanotubes are all metals in the absence of the E_{ext}, because the localized states result from the special geometry at $E_g = 0eV$. The metallic character does not change even in the presence of the perpendicular E_{ext}. Therefore, we chose to study armchair nanotubes in our study. This paper is structured as follows: In the "Computational methods" section, we briefly present the computational methods, followed by the discussion of the numerical results and their interpretations. Finally, the "Conclusions" section summarizes the discussions and the outcomes of this work.

Computational methods

The electronic and optical properties of the SWCNT/Carboxyl structure are determined based on DFT calculations using CASTEP code by OTFG ultrasoft pseudopotentials [14, 15]. Only the valence electrons (C $2s^2 2p^2$ and O $2s^2 2p^4$) are considered using ultrasoft pseudopotentials. In this study, the exchange–correlation energy employed using Perdew-Burke-Ernzerhof (PBE) functional is used within the generalized gradient approximation (GGA) [16, 17]. A plane-wave energy cut-off was set to 500 eV for all calculations [18].

The K-point of the Brillouin zone sampled is computed using $5 \times 5 \times 1$ gamma-centered Monkhorst–Pack grid during the geometry optimizations of the SWCNT/Carboxyl structure [19]. However, during all structural relaxations the convergence tolerance criteria for the geometry optimization was set to 2×10^{-6} eV/atom for energy. During the atomic relaxations the positions of atoms are optimized until convergence of the strength on each atom was less than 0.05 eV/Å and 0.03 Å for the displacement. The self-consistent field (SCF) convergence tolerance was set to 2×10^{-6} eV/atom. The maximum stress was set to 0.1 GPa.

In the present simulations, the SWCNT/Carboxyl structure was investigated using the CASTEP code. The system chosen for this test was a 52-atom that contains the H, O, and C atoms, their coordinates are shown in Table 1. In this atomic structure, the C(=O)OH group was deposited randomly on the side of the SWCNT sheet. The electrical and optical properties of the SWCNT/Carboxyl layer were obtained by applying E_{ext} in the z-direction with an intensity ranging from 0 V/Å to 0.3 V/Å. We construct an armchair carbon nanotube (SWCNT) with m = n = 6, bond length equal to 1.42 Å, and diameter d = 8.14 Å with supercell range (A = 1, B = 1, C = 2) substituted by the carboxyl group as shown in Figure 1. The Kohn–Sham Hamiltonian is represented by a set of plane waves in CASTEP. As a result, its periodicity is implicit. In order to study the SWCNT/Carboxyl structure using CASTEP, it is necessary to treat it as a periodic system by assuming that it is in a box. It is not necessary to limit the size of the supercell, but using a large enough supercell to eliminate spurious interactions between periodic images is the simplest approach. The SWCNT/Carboxyl structure was placed inside the simulation cell. The dimensions of the cell were a = 11.483001 Å, b = 11.483001 Å, c = 4.919024 Å, α = β = 90°, and γ = 120° for optimized calculations.

Table 1 The coordinates of C, O, and H atoms in supercell of the SWCNT/Carboxyl

Element	Atom number	Fractional coordinates of atoms		
		u	v	w
H	1	0.162102	0.897179	0.679921
C	1	0.895224	0.745306	0.028855
C	2	0.883075	0.799970	0.278983
C	3	0.781359	0.907277	0.028214
C	4	0.827413	0.883450	0.278549
C	5	0.380584	0.770624	0.027299
C	6	0.659727	0.907520	0.027909
C	7	0.590962	0.887789	0.277744
C	8	0.255630	0.649089	0.027011
C	9	0.201505	0.583472	0.274499
C	10	0.450718	0.817891	0.278651
C	11	0.107381	0.375798	0.027601
C	12	0.127060	0.444867	0.279282
C	13	0.228969	0.106038	0.028185
C	14	0.098115	0.251095	0.027715
C	15	0.111753	0.197796	0.279038
C	16	0.348496	0.101989	0.028017
C	17	0.416145	0.116000	0.277964
C	18	0.179113	0.125093	0.278442
C	19	0.626180	0.221797	0.028044
C	20	0.556040	0.175612	0.277917
C	21	0.886289	0.619684	0.028531
C	22	0.750202	0.340995	0.028072
C	23	0.798824	0.410187	0.278505
C	24	0.864908	0.549978	0.278740
C	25	0.893132	0.744341	0.529432
C	26	0.884771	0.801280	0.779139
C	27	0.781338	0.907443	0.528775
C	28	0.828476	0.884753	0.778699
C	29	0.384150	0.774621	0.527574
C	30	0.660150	0.908430	0.527963
C	31	0.590889	0.888253	0.777890
C	32	0.235762	0.666170	0.526780
C	33	0.197509	0.585155	0.781174
C	34	0.450752	0.818689	0.776371
C	35	0.096970	0.372993	0.528969
C	36	0.123324	0.444763	0.777488
C	37	0.227984	0.104169	0.528125
C	38	0.092138	0.247991	0.528556
C	39	0.109873	0.196270	0.777207
C	40	0.348806	0.102033	0.528038
C	41	0.416362	0.116085	0.778188
C	42	0.178281	0.124146	0.777957
C	43	0.625868	0.221718	0.528114
C	44	0.556033	0.175150	0.778145
C	45	0.883737	0.618565	0.529399
C	46	0.749679	0.340953	0.528677
C	47	0.800518	0.409699	0.778450
C	48	0.867623	0.550459	0.779002
C	49	0.176142	0.761312	0.498568
O	1	0.195279	0.834852	0.722148
O	2	0.131492	0.773809	0.284933

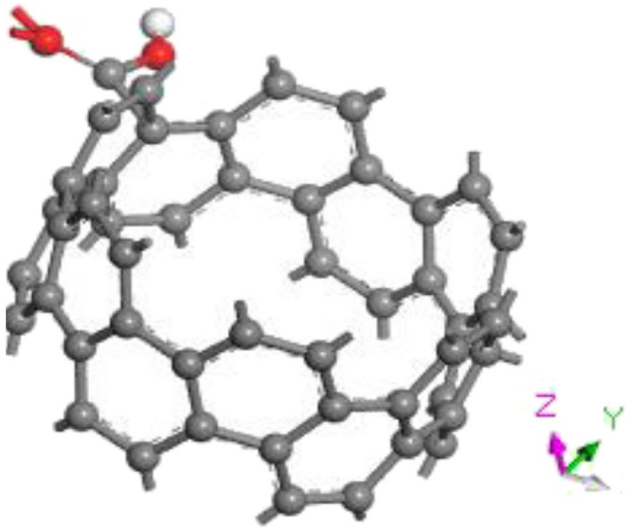

Fig. 1 Crystal structure of the SWCNT/Carboxyl; the gray sphere represents the carbon atom; the second blanch and red spheres represent hydrogen and oxygen atoms respectively

Results and discussions

Electronic structure

Optical gap

Applying an E_{ext} on a material is a method for controlling its bandgap. However, in the case of the SWCNT/Carboxyl, the band structures are calculated along the high symmetry directions in the Brillouin zone; as plotted in Figure 2. The band structures show that the conduction band minimum and the valence band maximum are located at various points of the Brillouin zone which indicate that the SWCNT/Carboxyl structure has a direct bandgap (see Figure 2). The bandgap of the SWCNT/Carboxyl decreases from 0.384 eV to 0.119 eV as the applied E_{ext} in the z-direction rises from 0 V/Å to 0.3 V/Å, as shown in Figure 3. These results show the bandgap tightening by the E_{ext} effect. The response of the SWCNT/Carboxyl bandgap under an $E_{ext} - field$ applied in the z-direction is used to facilitate the modulation of this electronic property.

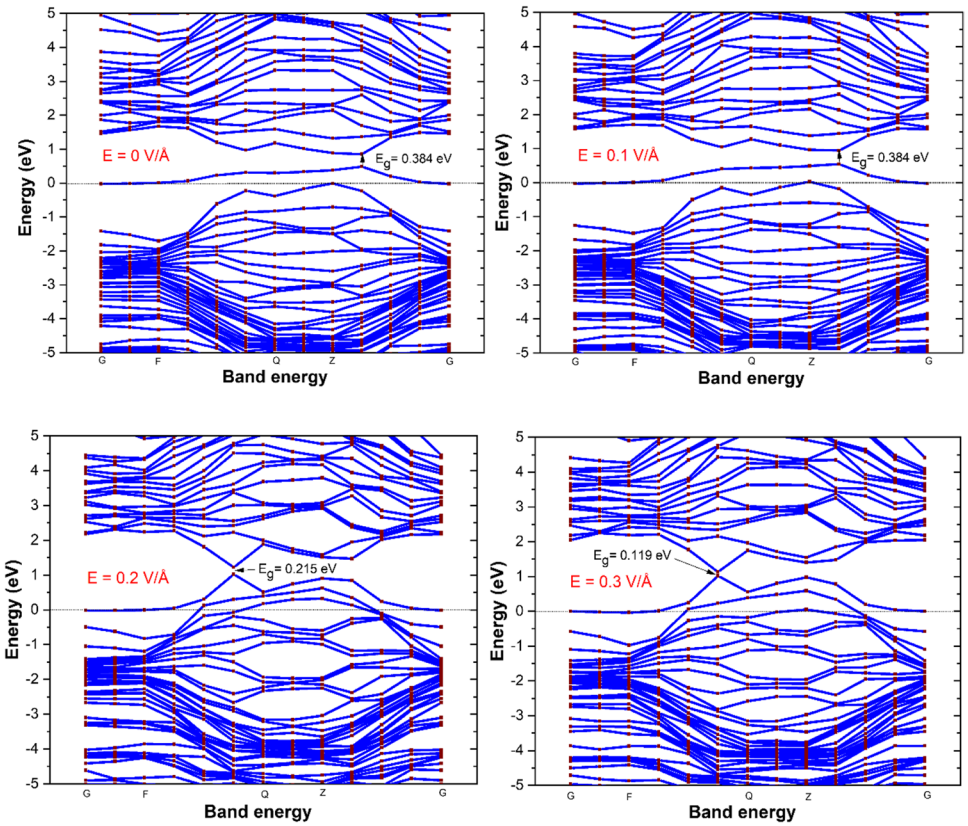

Fig. 2 Band structures of the SWCNT/Carboxyl under the E_{ext} applied in the z-direction

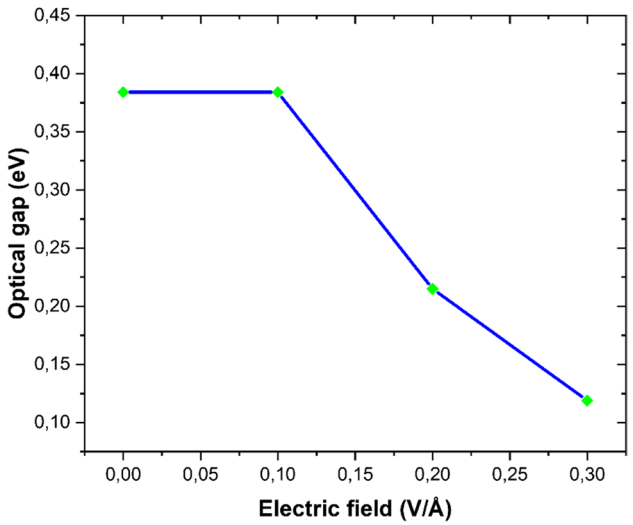

Fig. 3 Bandgap energy variation as a function of the E_{ext}

It is clear from Figure 3 that the SWCNT/Carboxyl structure exhibit a decrease in the bandgap energy when we introduced the E_{ext}, indicating the semiconducting property of this 1D material. The effect of the E_{ext} on the bandgap near Fermi level can be summarized as follows: Both conduction and valence bands did not change for an $E_{ext} = 0.1V/\text{Å}$ indicating that this value of E_{ext} does not influence the valence electrons of the SWCNT/Carboxyl structure. Both conduction and valence bands upshift and get closer for an $E_{ext} = 0.2V/\text{Å}$. The conduction band downshifts and the valence band remains almost fixed for closing the bandgap under an $E_{ext} = 0.3V/\text{Å}$ value. The presence of perturbing potential is bigger than 0.1 V/Å can lead to mixing the energy states and breaking the symmetry of the SWCNT/Carboxyl structure. These results indicate that the SWCNT/Carboxyl behaves as a semiconductor material with bandgap modulated by the E_{ext}.

Density of stats

The concept of density of states corresponds to the number of allowed electron energy states per unit of energy interval around an energy E. The TDOS and PDOS of the SWCNT/Carboxyl structure under the E_{ext} with the varying intensity from 0 V/Å to 0.3 V/Å applied in the z-direction are plotted in Figure 4 and Figure 5, respectively. The TDOS near the Fermi level exhibits a low population because of the semiconducting character of the SWCNT/Carboxyl material. The occupation probability of the electronic states increases for the electrons and decreases for the holes around the Fermi level by the E_{ext} applied on the SWCNT/Carboxyl in the

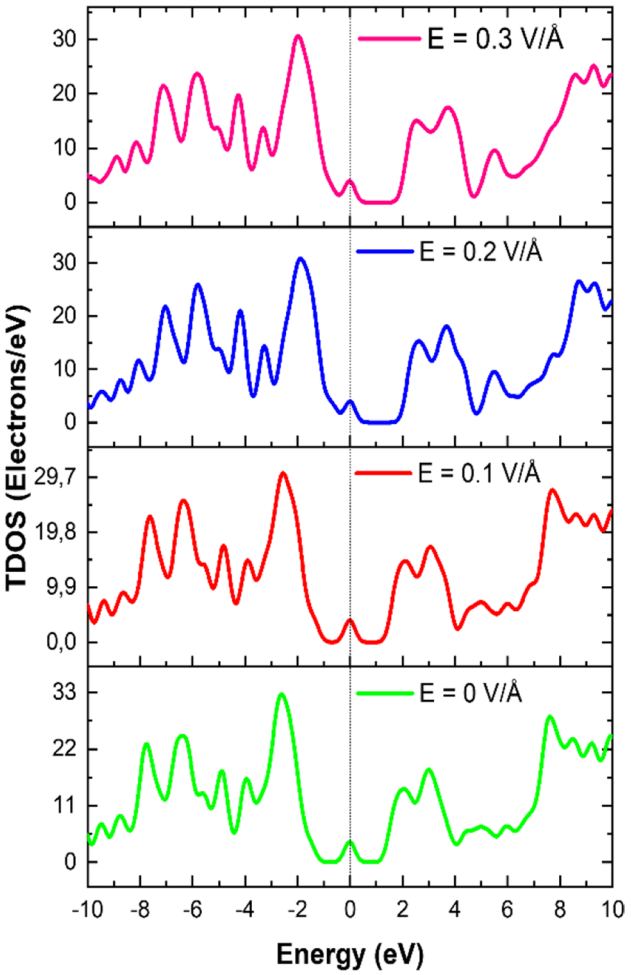

Fig. 4 Calculated TDOS as a function of the energy of the SWCNT/Carboxyl under the E_{ext}

z-direction (see Figure 4). These results confirm the bandgap energy reduction by the effect of E_{ext}.

The PDOS which is essentially the local DOS for each individual atom in the SWCNT/Carboxyl can provide additional insight into any observed changes in electronic structure, as shown in Figure 5. The states of all atoms around the Fermi level originate primarily from the valence electron orbitals of the SWCNT/Carboxyl structure. As a result, we have emphasized on them when mapping the PDOS. The peaks of PDOS-s intensities increase around the Fermi level by the E_{ext} effect, this implies that the chance of 2p orbitals being occupied by electrons from the 2 s shell has increased.

When applying the E_{ext}, the carbon atoms of the SWCNT gain electrons while the oxygen atoms of the carboxyl group lose them. The electrons gained by carbon atoms are attributed to their 2p orbitals. Both electron numbers, lost by oxygen atoms and those gained by carbon atoms of the SWCNT/Carboxyl, increase when increasing the E_{ext}. The electron transfer behavior can be studied by electron density difference, as plotted in Figure 5. The results indicate the strong effect of E_{ext} on electronic properties of the SWCNT/Carboxyl material.

Optical properties

Absorption In the present study, we present the variation of the SWCNT/Carboxyl structure's absorption coefficient under the applied E_{ext} in the z-direction as plotted from 0 to 8 eV range (see Figure 6). The absorption spectrum without the effect of the E_{ext} consists of two peaks with different intensities. A first peak appears at 1.735 eV and the second peak with a sharper intensity is located at 4.411 eV. The origin of these peaks arises from two important transitions that occur between the electronic states. The first peak corresponds to the transition of electrons from occupied states, n, to unoccupied states, n*, in the conduction band. The second broad peak corresponds to electron transition of C–C bonds in sp^2 hybrid regions; from π-π* states near the Fermi level. According to the absorption spectra, the SWCNT/Carboxyl exhibits strong light absorption in both UV and visible ranges. The intensity of absorption peaks in the UV range decreases due to increased interactions between the valence electrons and nucleus in the SWCNT/Carboxyl material under the E_{ext}. Additionally, the first absorption's peak intensity, located in the visible range, increases proportionally with E_{ext} due to the decrease of bandgap energy due to the electrons that moved from the valence band to the conduction band.

The application of the E_{ext} on the SWCNT/Carboxyl in the z-direction leads to a redshift of the absorption edge. This result, is confirming the decrease of bandgap energy. The E_{ext} can be effectively used to modify the absorption of the SWCNT/Carboxyl. Moreover, the E_{ext} effect allows us to boost the SWCNT/Carboxyl material's great light absorbing capacity, which is critical for photo-induced applications such as solar cells.

Dielectric function

The complex frequency is dependent on the dielectric function, $\varepsilon(\omega)$, that can be used to describe the optical properties of the 1D material. It can determine the dispersion effects by its real part $\varepsilon_1(\omega)$ and the absorption by its imaginary part $\varepsilon_2(\omega)$. The complex dielectric function $\varepsilon(\omega)$ is the sum of real and imaginary part as in Eq. (2):

$$\varepsilon(\omega) = \varepsilon_1(\omega) + i\varepsilon_2(\omega) \tag{2}$$

In the present work, the $\varepsilon(\omega)$ of the SWCNT/Carboxyl under the E_{ext} applied in the z-direction was calculated from 0 to 8 eV range and presented in Figure 7. The incident photons promote electrons to empty conduction states,

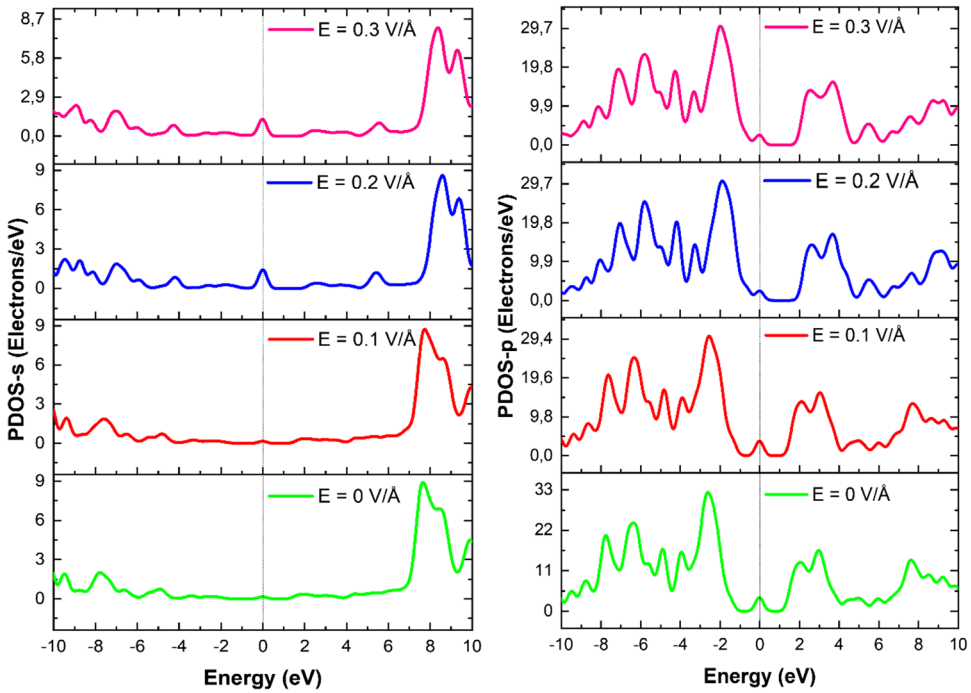

Fig. 5 Calculated PDOS-s and PDOS-p as a function of the energy of the SWCNT/Carboxyl under the E_{ext}

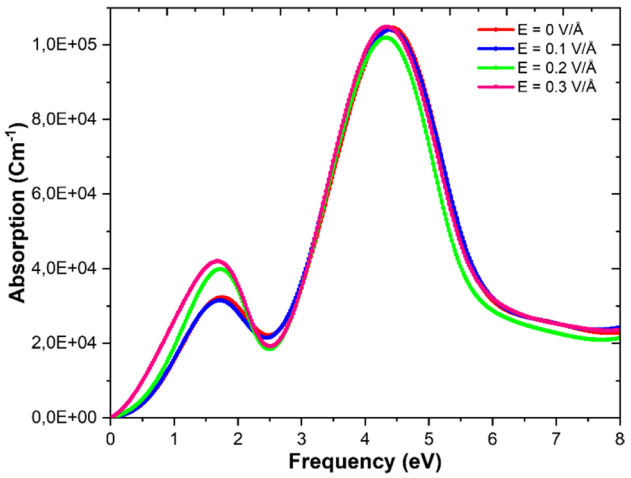

Fig. 6 The absorption coefficient of the SWCNT/Carboxyl structure under the E_{ext} applied in the z-direction

leaving holes behind in the occupied valence states. The excitation of free carriers affects the dielectric function by absorbing photons. In addition, the dielectric function of excited states still depends on the average excited state gap E_g [20]. At low energies, $\varepsilon(\omega)$ is associated with electronic intraband transitions in the conduction band. In this spectral range, the optical response is dominated by the free electron behavior. Although, at higher energies, $\varepsilon(\omega)$ reflects the electronic interband transitions. The application of the E_{ext} in the z-direction of the SWCNT/Carboxyl leads to an intensity decrease for the peaks of $\varepsilon_1(\omega)$ in the visible range, due to the increase in the interaction between the electrons and the incident photons. As a result, the dispersion of visible light in this material is decreased. The $\varepsilon_2(\omega)$ part has two peaks in the 0 to 8 eV range that are always related to the electron excitation. Additionally, the peak intensities of $\varepsilon_2(\omega)$ increase in the visible range by the E_{ext} applied in the z-direction. These results show the remarkable enhanced abilities to absorb the photons by the SWCNT/Carboxyl material, in the visible range under the E_{ext} applied in the z-direction. Therfore, we can introduce the SWCNT/Carboxyl material in transparent conducting films and photovoltaic devices.

Refractive index

Propagation in absorbing materials can be described using a complex-value of refractive index $n^*(\omega)$. The imaginary part, $k(\omega)$, handles the decrease, while the real part $n(\omega)$ accounts for refraction [21]:

$$n^*(\omega) = n(\omega) + ik(\omega) \tag{3}$$

$$n(\omega) = \sqrt{\frac{|\varepsilon(\omega)| + \varepsilon_1(\omega)}{2}} \tag{4}$$

$$k(\omega) = \sqrt{\frac{|\varepsilon(\omega)| - \varepsilon_1(\omega)}{2}} \tag{5}$$

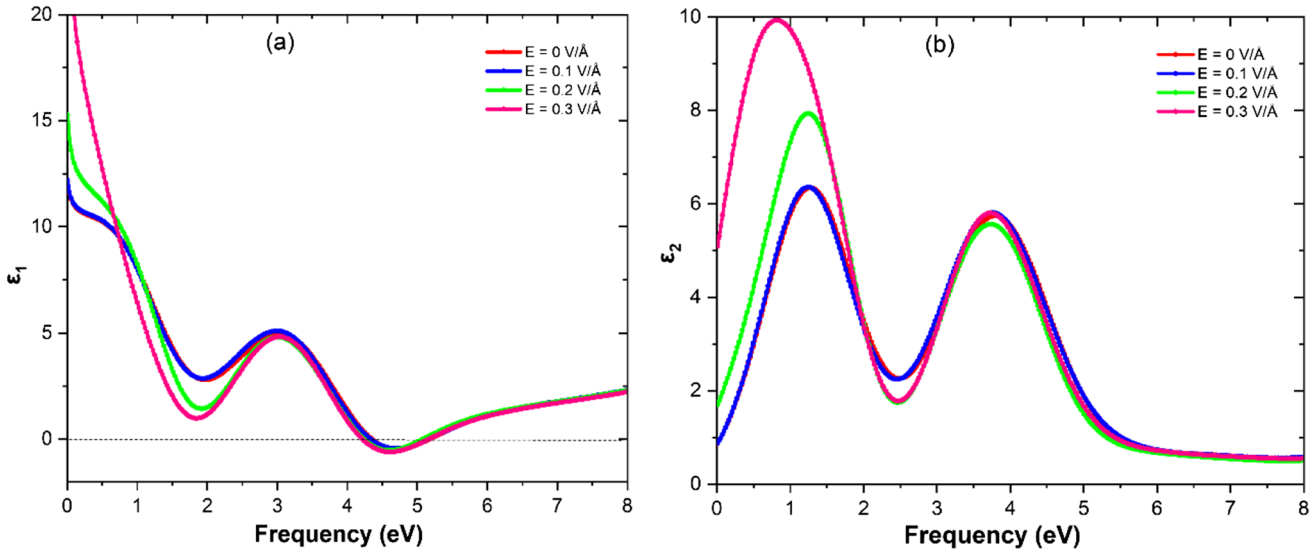

Fig. 7 Calculated $\varepsilon_1(\omega)$ and $\varepsilon_2(\omega)$ of the SWCNT/Carboxyl under the E_{ext} applied the in the z-direction

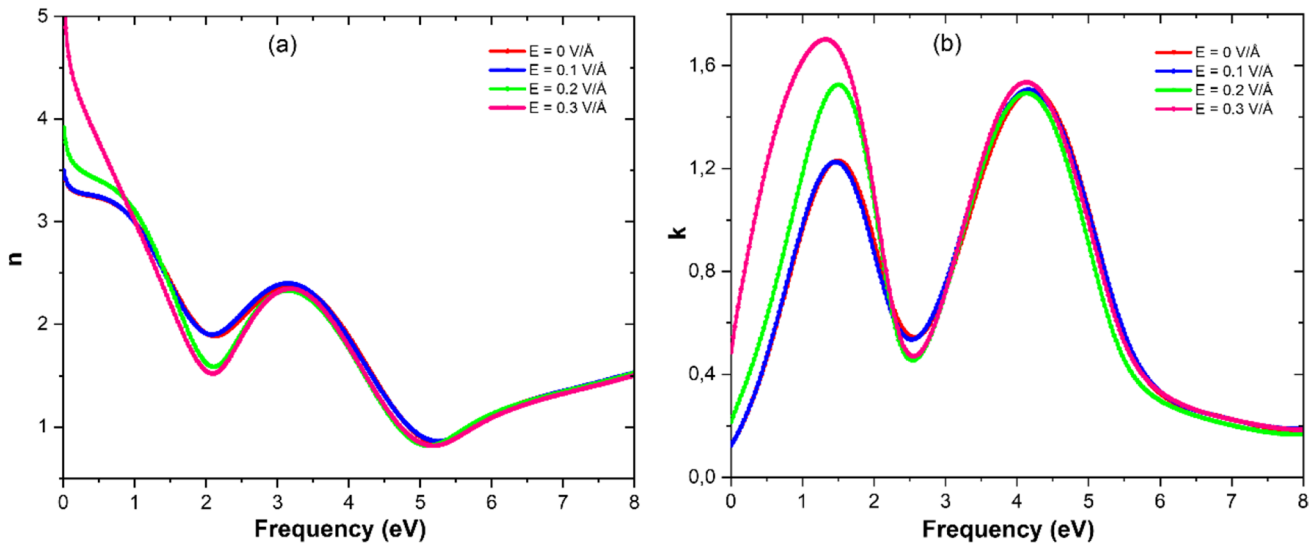

Fig. 8 Calculated $n(\omega)$ and $k(\omega)$ of the SWCNT/Carboxyl under the E_{ext}

The variation of refractive index, $n(\omega)$, and the extinction coefficient, $k(\omega)$, of the SWCNT/Carboxyl under the E_{ext} applied in the z-direction as a function of the frequency are calculated using CASTEP code and plotted in Figure 8. Both values $\varepsilon_1(0)$ and $n(0)$ validate the relation $n = \sqrt{\varepsilon_1}$ as presented in Table 2. The $n(\omega)$ part was varied as a function of the frequency under the E_{ext} applied on the SWCNT/Carboxyl structure. Hence, this material is a dispersive medium and its dispersion was influenced by the E_{ext}.

The refractive index of the SWCNT/Carboxyl under the E_{ext} applied in the z-direction is greater than 0.846, due to the incident photon energy $E = h\nu > 5.251eV$. This effect leads to create a reflexion of light on the particles inside the SWCNT/Carboxyl structure. The increase of the E_{ext} on the SWCNT/Carboxyl leads to a decrease in the visible range, $n(\omega)$, because of the increase of the interaction and the collision between the incident photons and electrons inside the

Table 2 Static dielectric constant $\varepsilon_1(0)$ and refractive index $n(0)$ of the SWCNT/Carboxyl

Parameters	$E_\perp$			
$E(V/Å)$	0	0.1	0.2	0.3
$n(0)$	3.485	3.493	3.913	5.217
$\varepsilon_1(0)$	12.130	12.189	15.271	26.981

SWCNT/Carboxyl material. As a result to this, the velocity of electrons ($v = \frac{c}{n}$) is increased. Besides, the $k(\omega)$ part increases in the visible region because of the decrease of the bandgap energy under the E_{ext} as plotted in Figure 8. The analysis of the graphs of $\varepsilon_2(\omega)$ and $k(\omega)$ parts, a similar physical behavior is observed in Figure 7 and Figure 8. These two physical quantities give information on the light absorption by the SWCNT/Carboxyl material.

Conductivity

It is interesting to know the complex optical conductivity $\sigma(\omega)$ of the SWCNT/Carboxyl material, because we can derive its valuable physical information. The conductivity $\sigma(\omega)$ is given by the following relations [22]:

$$\sigma(\omega) = \sigma_1(\omega) + i\sigma_2(\omega) \tag{6}$$

$$\sigma_1(\omega) = 2nk\left(\frac{\omega}{4\pi}\right) \tag{7}$$

$$\sigma_2(\omega) = \left[1 - \left(n^2 - k^2\right)\right]\left(\frac{\omega}{4\pi}\right) \tag{8}$$

The real $\sigma_1(\omega)$ and imaginary $\sigma_2(\omega)$ parts of the optical conductivity are calculated from the SWCNT/Carboxyl structure under the E_{ext} applied in the z-direction, as plotted in Figure 9. The first peak of $\sigma_1(\omega)$ appears at 1.536 eV which corresponds to the fundamental bandgap, due to the interband transitions of the valence electrons. The application of the E_{ext} on the SWCNT/Carboxyl structure in the z-direction leads to an increase in the $\sigma_1(\omega)$ part in the visible range, because of the increasing of electrons number as well as the decrease of the energy difference between the valence band and conduction band. The $\sigma_2(\omega)$ part has two peaks from the 0 to 8 eV range. The first peak has a negative value in the visible range, by reason of well-distributed charge in the SWCNT/Carboxyl material. The application of the E_{ext} increase the $\sigma_2(\omega)$ peaks in the visible range, due to the increased radiation scatterings; such as the visible light.

Loss function

The loss function describes the energy lost by an electron passing through a homogeneous dielectric material. From the real and imaginary parts of complex dielectric function, $L(\omega)$ can be easily obtained by [23]:

$$L(\omega) = -Im\left(\frac{1}{\varepsilon(\omega)}\right) = \frac{\varepsilon_2(\omega)}{\varepsilon_1^2(\omega) + \varepsilon_2^2(\omega)} \tag{9}$$

Calculated $L(\omega)$ functions of the SWCNT/Carboxyl structure under the E_{ext} applied in the z-direction are shown in Figure 10. The origin of several peaks of $L(\omega)$ is due to the collective excitations for various incident photons' frequencies. The $L(\omega)$ function has two peaks located at 2.044 and 5.406 eV, associated with the plasma frequency. These peaks indicate the maximum energy lost inside the SWCNT/Carboxyl material, by reason of the interaction of radiation (incident photons) with the different particles in SWCNT/Carboxyl material. In the visible range, the energy loss increases under the E_{ext} because of the increase in the absorption of photons by this material. A peak in the $L(\omega)$

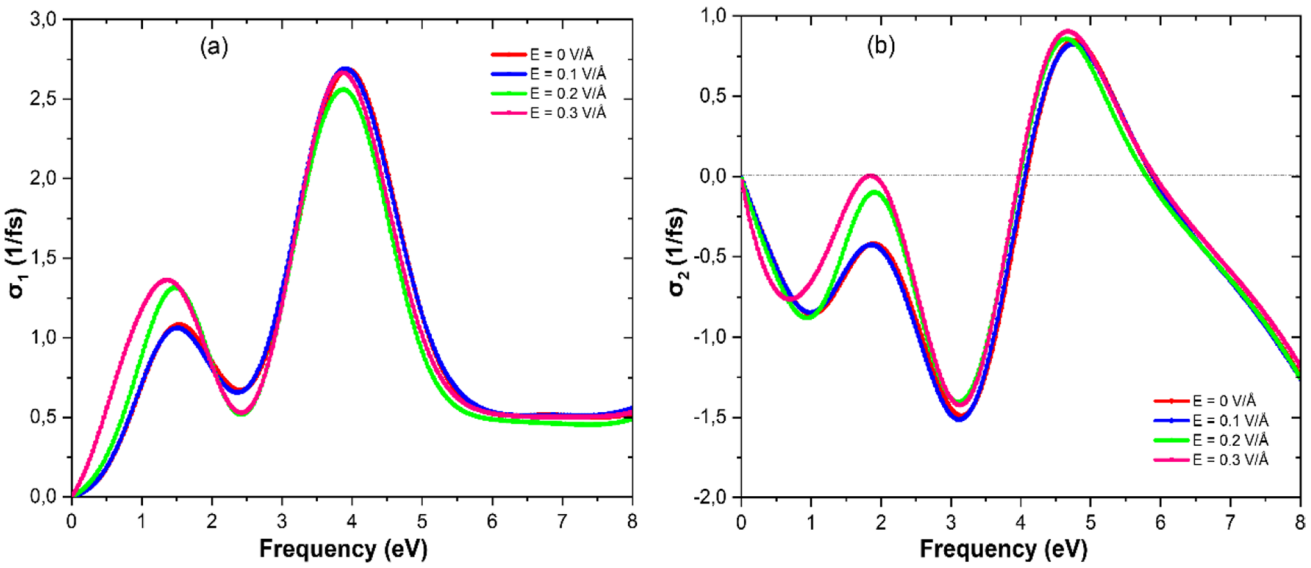

Fig. 9 Calculated σ of the SWCNT/Carboxyl structure under the E_{ext} applied in the z-direction

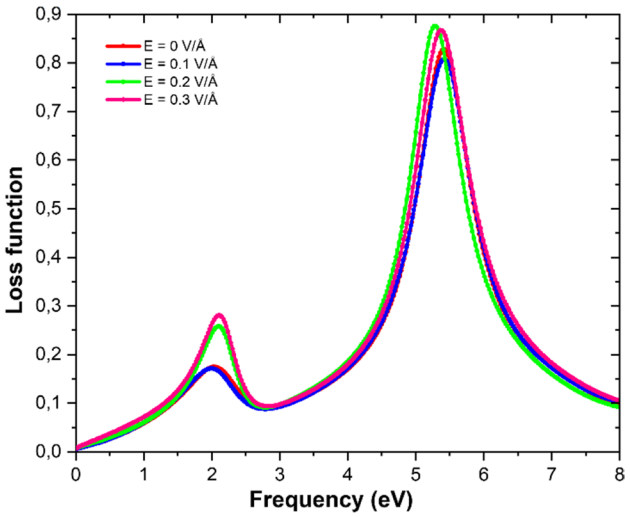

Fig. 10 Calculated $L(\omega)$ of the SWCNT/Carboxyl structure under the E_{ext}

function corresponds to a dip of the real part of the dielectric function (Figure 7 and Figure 10).

Conclusions

In this work, we have studied the electronic and optical properties of the SWCNT/Carboxyl structure, under the E_{ext} applied in the z-direction, by using the DFT calculations. The application of the E_{ext} produces new results in both band structure and optical properties of this 1D material. We have successfully reached a semiconducting behavior as well as a significant bandgap modification when applying the E_{ext}. We detected some alterations in dielectric function because of a lowering in bandgap energy. The intensity of absorption peak increases when the E_{ext} was applied in the z-direction of the SWCNT/Carboxyl. We have come to the conclusion that E_{ext} is a powerful tool to control electronic and optical properties of the SWCNT/Carboxyl material. These findings are a first step toward an experimental study of SWCNT/Carboxyl in a variety of applications, including optoelectronic devices.

Acknowledgements In conclusion, the authors sincerely thank all that contributed to this scientific work and particularly UNESCO UNISA Africa Chair in Nanosciences & Nanotechnology (U2ACN2), College of Graduate Studies, University of South Africa (UNISA), Pretoria, South Africa, and Sultan Moulay Slimane University Beni Mellal Morocco.

Author contribution The authors have approved the manuscript and agree with submission to your esteemed journal. All authors have participated in (a) conception and design, or analysis and interpretation of the data; (b) drafting the article or revising it critically for important intellectual content; and (c) approval of the final version.

Data availability All data generated or analyzed during this study are included in this published article.

Code availability We have used CASTEP code by OTFG ultrasoft pseudopotentials (Material Studio).

Declarations

Conflict of interest The authors declare no competing interests.

References

1. V. Lukose, R. Shankar, G. Baskaran, Novel electric field effects on landau levels in graphene, Phys. Rev. Lett. 98 (2007). https://doi.org/10.1103/PhysRevLett.98.116802.
2. Y. Yao, F. Ye, X.L. Qi, S.C. Zhang, Z. Fang, Spin-orbit gap of graphene: first-principles calculations, Phys. Rev. B - Condens. Matter Mater. Phys. 75 (2007) 1–4. https://doi.org/10.1103/PhysRevB.75.041401.
3. Balu R, Zhong X, Pandey R, Karna SP (2012) Effect of electric field on the band structure of graphene/boron nitride and boron nitride/boron nitride bilayers. Appl Phys Lett 100:3–6. https://doi.org/10.1063/1.3679174
4. H. Mehrez, A. Svizhenko, M.P. Anantram, M. Elstner, T. Frauenheim, Analysis of band-gap formation in squashed armchair carbon nanotubes, Phys. Rev. B - Condens. Matter Mater. Phys. 71 (2005) 1–7. https://doi.org/10.1103/PhysRevB.71.155421.
5. Orellana W, Fuentealba P (2006) Structural, electronic and magnetic properties of vacancies in single-walled carbon nanotubes. Surf Sci 600:4305–4309. https://doi.org/10.1016/j.susc.2006.01.158
6. Prabhu S, Bhaumik S, Vinayagam BK (2012) Finite element modeling and analysis of zigzag and armchair type single wall carbon nanotube. J Mech Eng Res 4:260–266. https://doi.org/10.5897/JMER12.025
7. Popov VN (2004) Carbon nanotubes: properties and application. Mater Sci Eng R Reports 43:61–102. https://doi.org/10.1016/j.mser.2003.10.001
8. Dresselhaus MS, Dresselhaus G, Saito R (1995) Physics of carbon nanotubes. Carbon N Y 33:883–891. https://doi.org/10.1016/0008-6223(95)00017-8
9. Yoosefian M, Etminan N (2016) Density functional theory (DFT) study of a new novel bionanosensor hybrid; tryptophan/Pd doped single walled carbon nanotube. Phys E Low-Dimensional Syst Nanostructures 81:116–121. https://doi.org/10.1016/j.physe.2016.03.009
10. Chełmecka E, Pasterny K, Kupka T, Stobiński L (2012) DFT studies of COOH tip-functionalized zigzag and armchair single wall carbon nanotubes. J Mol Model 18:2241–2246. https://doi.org/10.1007/s00894-011-1242-x
11. M.H. Majles Ara, Z. Dehghani, Improvement of the third order nonlinear optical properties of nematic liquid crystal under the influence of different compositional percentage of doped SWCNT and the external electric field, J. Mol. Liq. 275 (2019) 281–289. https://doi.org/10.1016/j.molliq.2018.11.069.
12. D. Singh, U. Bahadur Singh, M. Bhushan Pandey, R. Dabrowski, R. Dhar, Improvement of orientational order and display parameters of liquid crystalline material dispersed with single-wall carbon nanotubes, Mater. Lett. 216 (2018) 5–7. https://doi.org/10.1016/j.matlet.2017.12.099.
13. T. yu Tang, Y. Liu, X. feng Diao, Y. lin Tang, Study on conductivity properties and stability of NbAs based on first-principles,

Comput. Mater. Sci. 181 (2020) 109731. https://doi.org/10.1016/j.commatsci.2020.109731.
14. Delley B (1990) An all-electron numerical method for solving the local density functional for polyatomic molecules. J Chem Phys 92:508–517. https://doi.org/10.1063/1.458452
15. E.R. McNellis, J. Meyer, K. Reuter, Azobenzene at coinage metal surfaces: role of dispersive van der Waals interactions, Phys. Rev. B - Condens. Matter Mater. Phys. 80 (2009). https://doi.org/10.1103/PhysRevB.80.205414.
16. Perdew JP, Burke K, Ernzerhof M (1996) Generalized gradient approximation made simple. Phys Rev Lett 77:3865–3868. https://doi.org/10.1103/PhysRevLett.77.3865
17. Matsuda Y, Tahir-Kheli J, Goddard WA (2010) Definitive band gaps for single-wall carbon nanotubes. J Phys Chem Lett 1:2946–2950. https://doi.org/10.1021/jz100889u
18. V. Zólyomi, J. Kürti, First-principles calculations for the electronic band structures of small diameter single-wall carbon nanotubes, Phys. Rev. B - Condens. Matter Mater. Phys. 70 (2004) 1–8. https://doi.org/10.1103/PhysRevB.70.085403.
19. Hendrik J Monkhorst, J.D. Pack, Special points for Brillouin-zone integration Monkhorst and Pack, Phys. Rev. B. 13 (1976) 5188–5192. http://prb.aps.org/pdf/PRB/v13/i12/p5188_1.
20. Kim DH, Ehrenreich H, Runge E (1994) Solid State Commun 89:119
21. Lashgari H, Boochani A, Shekaari A, Solaymani S (2016) Applied Surface Science Electronic and optical properties of 2D graphene-like ZnS : DFT calculations. Appl Surf Sci 369:76–81. https://doi.org/10.1016/j.apsusc.2016.02.042
22. Gravier P, Sigrist M, Chassaing G (1977) Détermination de la conductivité optique de couches minces semi-transparentes. Opt Acta (Lond) 24:733–741. https://doi.org/10.1080/713819628
23. E.A. Taft, H.R. Philipp, Optical properties of graphite, Phys. Rev. 138 (1965). https://doi.org/10.1103/PhysRev.138.A197.